Acta Crystallographica Section C
**Crystal Structure Communications**
ISSN 0108-2701

# Conformation of *tert*-butoxycarbonyl-glycyl-dehydroalanyl-glycine methyl ester in the crystalline state and calculated in the gas phase

**Krzysztof Ejsmont,[a]* Roman Gajda[b] and Maciej Makowski[a]**

[a]Institute of Chemistry, University of Opole, Oleska 48, 45-052 Opole, Poland, and [b]Faculty of Chemistry, Adam Mickiewicz University, Grunwaldzka 6, 60-780 Poznań, Poland
Correspondence e-mail: eismont@uni.opole.pl

Received 19 October 2006
Accepted 5 December 2006
Online 13 January 2007

*tert*-Butoxycarbonylglycyl-dehydroalanyl-glycine methyl ester (systematic name: methyl {2-[(*tert*-butoxycarbonylamino)-acetamido]prop-2-enamido}acetate) ($Boc^0$-$Gly^1$-$\Delta Ala^2$-$Gly^3$-OMe), $C_{13}H_{21}N_3O_6$, has been structurally characterized by single-crystal X-ray diffraction and by density functional theory (DFT) calculations at the B3LYP/6–311+G** level. The peptide chain in both the solid-state and calculated structures adopts neither $\beta$ nor $\gamma$ turns. All amino acid residues in the tripeptide sequence are linked *trans* to each other. The bond lengths and valence angles of the amino acid units in the crystal structure and gas phase are comparable. However, the conformation of the third glycyl residue ($Gly^3$) is different in the crystalline state and in the gas phase. It is stabilized in the calculated structure by an additional intramolecular short contact between $Gly^3$ NH and methyl ester COMe groups.

## Comment

The $\alpha,\beta$-dehydroamino acids in peptides have been found to be responsible for the formation of derivatives of natural peptides with interesting biological activities (Jain & Chauhan, 1996). This is mainly based on the presence of a $C^{\alpha}{=}C^{\beta}$ double bond, which gives not only specific chemical properties, but also an inherent conformational preference. Therefore, $\alpha,\beta$-dehydroamino acid residues attract much interest as a significant element in secondary structure design (helices, sheets and turns) in peptides. Apart from the presence of the $C^{\alpha}{=}C^{\beta}$ bond, which introduces steric repulsions, an important role is also played by intramolecular N—H···O, N—H···N and C—H···O hydrogen bonds and N—H···$\pi$-electron cross conjugation (Sigh & Kaur, 1997; Venkatachalam, 1968; Perczel *et al.*, 1996; Vass *et al.*, 2003).

The title methyl ester, $Boc^0$-$Gly^1$-$\Delta Ala^2$-$Gly^3$-OMe, (I), represents an example of a peptide with a rigid central amino acid ($\Delta$Ala) placed between two flexible glycine residues. Dehydroalanine ($\Delta$Ala) is the simplest and most widespread $\alpha,\beta$-dehydroamino acid. The insertion of such a small molecule into a peptide chain may significantly change its properties, *e.g.* the insertion of a $\Delta$Ala residue into the chains of the tripeptides Gly-$\Delta$Ala-Gly and Gly-$\Delta$Ala-Phe or the tetrapeptides Gly-$\Delta$Ala-Phe-Gly and Gly-Gly-$\Delta$Ala-Phe has an influence on the binding abilities of these peptide ligands towards copper(II) ions (Świątek-Kozłowska *et al.*, 2000). Another example is the Gly-$\Delta$Ala-Gly-Phe-pNA tetrapeptide, which acts as a substrate of dipeptidyl-peptidase (cathepsin C), representing comparable activity to their classical counterparts (Makowski *et al.*, 2001).

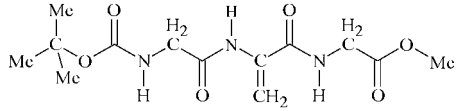

(I)

$\Delta$Ala adopts an almost planar conformation, with a *trans* orientation for the $\varphi$ and $\psi$ torsion angles, and induces an inverse $\gamma$ turn in the preceding residue. Similar effects were observed for linear dehydroalanine-containing peptides in solution and in the crystalline state. It seems that dehydroalanine exerts a powerful conformational influence independently of other constraints (Palmer *et al.*, 1992). A number of theoretical calculations have been devoted to the conformational preferences of $\Delta$Ala (*e.g.* Crisma *et al.*, 1999; Füzéry & Csizmadia, 2000; Rzeszotarska *et al.*, 2002; Siodłak *et al.*, 2004; Broda *et al.*, 2005). All these studies provide evidence that the fully extended conformation ($C_5$) is preferred by the $\Delta$Ala residue, with the $\varphi$, $\psi$ and $\omega$ backbone torsion angles very

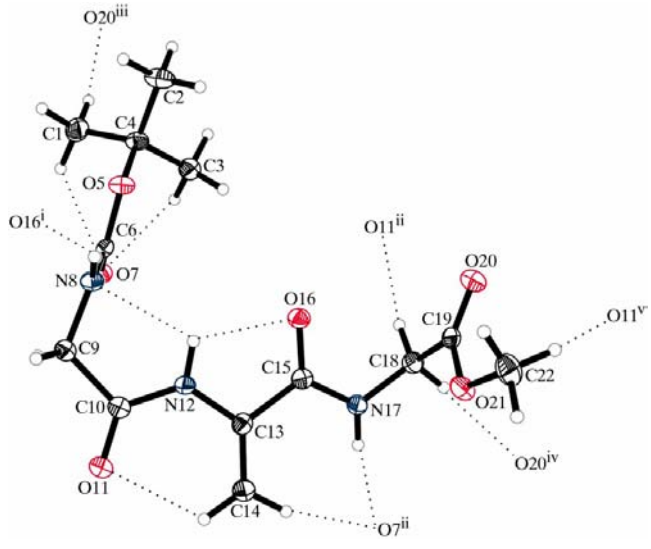


**Figure 1**
The molecular structure of (I), showing the intra- and intermolecular hydrogen-bonding scheme (dashed lines). Displacement ellipsoids are drawn at the 50% probability level and H atoms are shown as small spheres of arbitrary radii. [Symmetry codes: (i) $1-x, 1-y, -z$; (ii) $-x, 1-y, -z$; (iii) $1-x, 2-y, -z$; (iv) $-x, 1-y, -1-z$; (v) $x, y, z-1$.]

  DOI: 10.1107/S0108270106052590 

close to the *trans* orientation. This structure is stabilized by two types of intramolecular hydrogen bonds: $N_i—H\cdots O_i{=}C_i$, with a five-membered ring $C_5$ form, and $C^B_{i+1}—H\cdots O_i{=}C_i$, giving rise to a six-membered ring system. The conformational map calculated for Ac-ΔAla-NHMe reveals four minima located at values of the $\varphi$ and $\psi$ angles of around 180 or 0°. The lowest-energy conformer presents the fully extended structure, with $\varphi$ and $\psi$ torsion angles of 180 and 169°, respectively.

The conformation of (I) in the crystal structure, with the atom-numbering scheme, is shown in Fig. 1. This conformation is stabilized by both inter- and intramolecular hydrogen bonds and short contacts, and details of these are given in Tables 1 and 3. The similar tripeptide Boc-Gly-ΔPhe-Gly-OMe forms a type II$\beta$ turn, with an intramolecular N—H···O hydrogen bond between the third and first peptide units. The $C^\alpha_1\cdots C^\alpha_3$ distance is 5.387 (4) Å (Główka, 1988). The analogous distance in (I) is 7.038 (2) Å, which is insufficient for considering the secondary structure of (I) as a $\beta$ turn. Additionally, the 1←4 ($C_{10}$) and 1←3 ($C_7$) intramolecular hydrogen bonds, which are characteristic for $\beta$ and $\gamma$ turns, respectively, are not present.

The calculated conformation of (I) is shown in Fig. 2. This is the lowest-energy conformation of this compound in the gas phase. On the basis of the hydrogen-bonding backbone and the values of the $\varphi$ and $\psi$ torsion angles, the conformation of (I) in the gas phase could not be assigned to either $\beta$ or $\gamma$ turns. Table 2 lists the bond lengths and angles of the title compound in the crystal structure and calculated by the DFT method. All bond distances and valence angles are in good agreement with those observed in other peptides containing the ΔAla and Gly residues (Crisma *et al.*, 1999; Rzeszotarska *et al.*, 2002; Ajo *et al.*, 1979; Palmer *et al.*, 1992; Padmanabhan *et al.*, 1992; Piazzesi *et al.*, 1993). There are no significant differences between the bond lengths and angles of this tripeptide in the solid state and in the calculated structure; the differences do not exceed 0.04 Å for bond distances and 2° for bond angles.

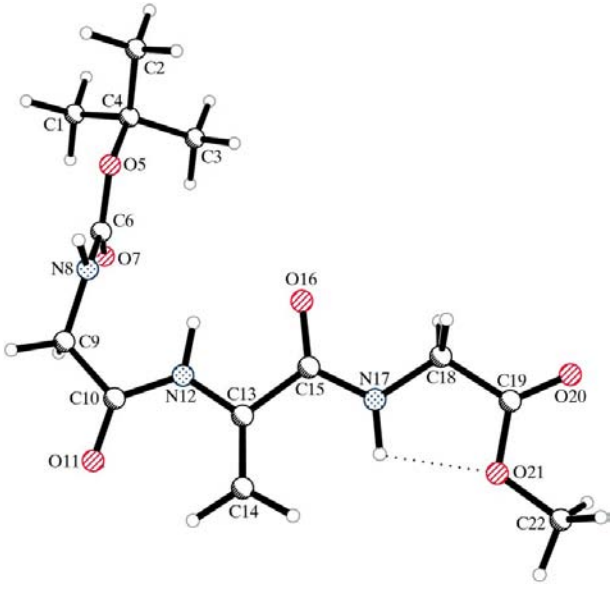


**Figure 2**
The molecular structure of (I) calculated by DFT, showing the intramolecular hydrogen bond (dotted line).

In both the solid state and the gas phase, the $Gly^1$-$\Delta Ala^2$ fragment of (I) adopts the fully extended conformation, with $\varphi$ and $\psi$ angles of around 180 and −170°, respectively. The planarity of this fragment is stabilized by intramolecular C14—H14*B*···O11, N12—H12···O16 and N12—H12···N8 hydrogen bonds and short contacts. Additionally, the coplanarity of the $Gly^1$-$\Delta Ala^2$ residue favours $\pi$-conjugation of the C13=C14 double bond with neighbouring amide bonds.

The differences between both the solid state and the gas phase of (I) become clearly visible when the torsion angles and intermolecular hydrogen bonds are considered. There are two places in the structure where these differences are particularly marked. One of these is the $Gly^1$ residue. The value of $\varphi_1$ which characterizes this residue increases from 89.0 (1)° in the crystal structure to 116° in the gas phase. More significant differences in conformation are observed in the $Gly^3$ residue. The value of the C15—N17—C18—C19 torsion angle which characterizes this residue in the crystal structure is 69.7 (1)°, while in the gas phase this angle increases by more than 100° to 176.84°, due to the fact that the $Gly^3$ and OMe residues become nearly coplanar. This conformational change is stabilized by an intramolecular N17—H17···O21 short contact (Table 3) observed only in the calculated structure.

Because of many competitive intermolecular hydrogen bonds, in the crystal structure of (I) there is a relatively large rotation of the N17—C18 bond (over 100°) and a slightly smaller rotation of the C18—C19 bond. A relatively strong N17—H17···$O7^{ii}$ hydrogen bond (which causes the molecules to arrange in a head-to-tail fashion) is present in the crystal structure of (I), as well as two others, *viz*. C18—H18*A*···$O11^{ii}$ and C18—H18*B*···$O20^{iv}$. Apart from these hydrogen bonds, there are also other intermolecular interactions, but only these hydrogen bonds cause the non-planarity of this residue in the crystal structure.

In similar compounds containing the Gly-OMe residue, such as ethyl (4-bromo-1*H*-pyrrole-2-carboxamido)acetate (Zeng, 2005), *N*-[*tert*-butoxycarbonylglycyl-(*Z*)-$\alpha$,$\beta$-dehydrophenylalanylglycyl-(*E*)-$\alpha$,$\beta$-dehydrophenylalanyl]glycine methyl ester dihydrate (Makowski *et al.*, 2006), 4,5-bis-[(ethoxyglycyl)carbonyl]-1*H*-imidazole and 4-ethoxycarbonyl-5-[(methoxyglycyl)carbonyl]-1*H*-imidazole (Baures *et al.*, 2002) and *tert*-butoxycarbonyl-glycyl-dehydrophenylalanyl-glycine methyl ester (Główka, 1988), the analogous torsion angles are −66.67, 135.24, 94.62, −92.24 and 71.67°, respectively. This indicates that this fragment is usually twisted in the crystal structure.

## Experimental

The title compound was synthesized by the reaction of Boc-Gly-ΔAla (after activation with *N*,*N*′-dicyclohexylcarbodiimide and 1-hydroxy-

benzotriazole) with Gly-OMe at room temperature for 24 h (Makowski *et al.*, 1986). Crystals of (I) suitable for X-ray crystal structure analysis were grown from a $CHCl_3$–MeOH–hexane (1:1:4) solution.

*Crystal data*

$C_{13}H_{21}N_3O_6$
$M_r$ = 315.33
Triclinic, $P\overline{1}$
$a$ = 8.6343 (14) Å
$b$ = 8.7713 (14) Å
$c$ = 11.2379 (15) Å
$\alpha$ = 110.158 (13)°
$\beta$ = 98.428 (12)°
$\gamma$ = 100.631 (14)°
$V$ = 764.6 (2) Å$^3$
$Z$ = 2
$D_x$ = 1.370 Mg m$^{-3}$
Mo $K\alpha$ radiation
$\mu$ = 0.11 mm$^{-1}$
$T$ = 100.0 (1) K
Cube, colourless
0.51 × 0.48 × 0.46 mm

*Data collection*

Oxford Xcalibur diffractometer
$\omega$ scans
7435 measured reflections
3000 independent reflections
2676 reflections with $I > 2\sigma(I)$
$R_{int}$ = 0.022
$\theta_{max}$ = 26.0°

*Refinement*

Refinement on $F^2$
$R[F^2 > 2\sigma(F^2)]$ = 0.031
$wR(F^2)$ = 0.082
$S$ = 1.08
3000 reflections
284 parameters
All H-atom parameters refined
$w = 1/[\sigma^2(F_o^2) + (0.0442P)^2 + 0.1565P]$ where $P = (F_o^2 + 2F_c^2)/3$
$(\Delta/\sigma)_{max} < 0.001$
$\Delta\rho_{max}$ = 0.23 e Å$^{-3}$
$\Delta\rho_{min}$ = −0.21 e Å$^{-3}$
Extinction correction: *SHELXL97* (Sheldrick, 1997)
Extinction coefficient: 0.021 (3)

**Table 1**
Comparison of selected geometric data for (I) (Å, °) from X-ray and calculated (DFT) data.

| | X-ray | DFT |
|---|---|---|
| C6—N8 | 1.345 (2) | 1.377 |
| N8—C9 | 1.435 (1) | 1.449 |
| C9—C10 | 1.520 (2) | 1.535 |
| C10—O11 | 1.212 (1) | 1.219 |
| C10—N12 | 1.347 (1) | 1.367 |
| N12—C13 | 1.394 (1) | 1.398 |
| C13—C14 | 1.319 (2) | 1.341 |
| C13—C15 | 1.495 (2) | 1.513 |
| C15—O16 | 1.232 (1) | 1.228 |
| C15—N17 | 1.328 (1) | 1.355 |
| N17—C18 | 1.442 (1) | 1.451 |
| | | |
| O11—C10—N12 | 124.8 (1) | 124.88 |
| O11—C10—C9 | 120.2 (1) | 119.98 |
| N12—C10—C9 | 114.95 (9) | 115.14 |
| C10—N12—C13 | 127.5 (1) | 128.05 |
| C14—C13—N12 | 125.9 (1) | 125.97 |
| C14—C13—C15 | 124.3 (1) | 124.30 |
| N12—C13—C15 | 109.74 (9) | 109.70 |
| O16—C15—N17 | 121.4 (1) | 122.17 |
| O16—C15—C13 | 120.1 (1) | 120.26 |
| N17—C15—C13 | 118.45 (9) | 117.57 |
| C15—N17—C18 | 118.66 (9) | 120.57 |
| N17—C18—C19 | 114.34 (9) | 113.79 |
| | | |
| O5—C6—N8—C9 ($\omega_0$) | 173.55 (9) | 169.68 |
| C6—N8—C9—C10 ($\varphi_1$) | 89.0 (1) | 116.90 |
| N8—C9—C10—N12 ($\psi_1$) | −2.0 (1) | −14.38 |
| C9—C10—N12—C13 ($\omega_1$) | −172.6 (1) | −179.52 |
| C10—N12—C13—C15 ($\varphi_2$) | 176.3 (1) | 179.97 |
| N12—C13—C15—N17 ($\psi_2$) | −171.84 (9) | −166.48 |
| O16—C15—N17—C18 | −0.5 (2) | 0.09 |
| C13—C15—N17—C18 ($\omega_2$) | 179.82 (9) | 179.78 |
| C15—N17—C18—C19 ($\varphi_3$) | 69.7 (1) | 176.84 |
| N17—C18—C19—O20 | −140.0 (1) | −176.61 |
| N17—C18—C19—O21 ($\psi_3$) | 43.1 (1) | 3.88 |

**Table 2**
Comparison of intramolecular hydrogen-bonding and short-contact geometry in (I) (Å, °) from X-ray and calculated (DFT) data.

| $D$—H···$A$ | $D$—H | H···$A$ | $D$···$A$ | $D$—H···$A$ |
|---|---|---|---|---|
| N12—H12···O16† | 0.87 (1) | 2.14 (1) | 2.602 (1) | 112 (1) |
| ‡ | 1.02 | 2.12 | 2.63 | 109 |
| N12—H12···N8† | 0.87 (1) | 2.29 (1) | 2.718 (1) | 110 (1) |
| ‡ | 1.02 | 2.30 | 2.73 | 108 |
| C1—H1*A*···O7† | 0.97 (1) | 2.56 (1) | 3.109 (2) | 116 (1) |
| ‡ | 1.09 | 2.46 | 3.052 | 113 |
| C3—H3*A*···O7† | 0.98 (1) | 2.57 (1) | 2.949 (2) | 103.1 (9) |
| ‡ | 1.09 | 2.46 | 3.049 | 113 |
| C14—H14*B*···O11† | 0.96 (2) | 2.29 (2) | 2.867 (2) | 118 (1) |
| ‡ | 1.08 | 1.26 | 2.910 | 117 |
| N17—H17···O21‡ | 1.01 | 2.19 | 2.628 | 105 |

† Values from X-ray data. ‡ Values from DFT calculations.

**Table 3**
Hydrogen-bond and short-contact geometry (Å, °).

| $D$—H···$A$ | $D$—H | H···$A$ | $D$···$A$ | $D$—H···$A$ |
|---|---|---|---|---|
| N8—H8···O16$^{i}$ | 0.87 (2) | 1.97 (2) | 2.834 (1) | 173 (1) |
| N17—H17···O7$^{ii}$ | 0.87 (2) | 2.10 (2) | 2.944 (1) | 167 (1) |
| C1—H1*B*···O20$^{iii}$ | 0.99 (2) | 2.48 (2) | 3.434 (2) | 161 (1) |
| C14—H14*A*···O7$^{ii}$ | 0.98 (2) | 2.54 (2) | 3.439 (2) | 154 (1) |
| C18—H18*A*···O11$^{ii}$ | 0.97 (1) | 2.68 (1) | 3.240 (2) | 117.6 (9) |
| C18—H18*B*···O20$^{iv}$ | 0.97 (2) | 2.49 (2) | 3.259 (1) | 137 (1) |
| C22—H22*A*···O11$^{v}$ | 0.97 (2) | 2.49 (2) | 3.459 (2) | 177 (1) |

Symmetry codes: (i) $-x+1, -y+1, -z$; (ii) $-x, -y+1, -z$; (iii) $-x+1, -y+2, -z$; (iv) $-x, -y+1, -z-1$; (v) $x, y, z-1$.

The geometry of (I) in the crystalline state was used as the starting structure for full optimization using standard density functional theory (DFT) employing the B3LYP hybrid function (Becke, 1988, 1993; Lee *et al.*, 1988) at the 6–311+G** level of theory, with no imaginary frequencies. The calculations were carried out using *GAUSSIAN03* (Frisch *et al.*, 2004). H atoms were located in a difference Fourier map and refined freely; refined C—H and N—H distances are in the ranges 0.956 (16)–1.002 (16) and 0.866 (15)–0.874 (14) Å, respectively.

Data collection: *CrysAlis CCD* (Oxford Diffraction, 2002); cell refinement: *CrysAlis RED* (Oxford Diffraction, 2002); data reduction: *CrysAlis RED*; program(s) used to solve structure: *SHELXS97* (Sheldrick, 1997); program(s) used to refine structure: *SHELXL97* (Sheldrick, 1997); molecular graphics: *SHELXTL* (Sheldrick, 1990); software used to prepare material for publication: *SHELXL97*.

The authors gratefully acknowledge the Academic Computer Centre CYFRONET AGH of Kraków for grant No. MNiI/SGI2800/UOpolski/007/2005.

Supplementary data for this paper are available from the IUCr electronic archives (Reference: AV3051). Services for accessing these data are described at the back of the journal.

## References

Ajo, D., Granozzi, G., Tondello, E., Pra, A. D. & Zanotti, G. (1979). *J. Chem. Soc. Perkin Trans. 2*, pp. 927–929.
Baures, P. W., Rush, J. R., Wiznycia, A. V., Desper, J., Helfrich, B. A. & Beatty, A. M. (2002). *Cryst. Growth Des.* **2**, 653–664.
Becke, A. D. (1988). *Phys. Rev. A.* **38**, 3098–3100.

Becke, A. D. (1993). *J. Chem. Phys.* **98**, 5648–5652.
Broda, M. A., Rospenk, M., Siodłak, D. & Rzeszotarska, B. (2005). *J. Mol. Struct.* **740**, 17–24.
Crisma, M., Formaggio, F., Toniolo, C., Yoshikawa, T. & Wakamiya, T. (1999). *J. Am. Chem. Soc.* **121**, 3272–3278.
Frisch, M. J. *et al.* (2004). *GAUSSIAN03*. Revision C.02. Gaussian Inc., Pittsburgh, Pennsylvania, USA.
Füzéry, A. K. & Csizmadia, I. G. (2000). *J. Mol. Struct. (Theochem)*, **501–502**, 539–547.
Główka, M. L. (1988). *Acta Cryst.* C**44**, 1639–1641.
Jain, R. & Chauhan, V. S. (1996). *Biopolymers*, **40**, 105–119.
Lee, C., Yang, W. & Parr, R. G. (1988). *Phys. Rev. B*, **37**, 785–789.
Makowski, M., Lisowski, M., Maciąg, A. & Lis, T. (2006). *Acta Cryst.* E**62**, o807–o810.
Makowski, M., Pawełczak, M., Latajka, R., Nowak, K. & Kafarski, P. (2001). *J. Pept. Sci.* **7**, 141–145.
Makowski, M., Rzeszotarska, B., Kubica, Z., Pietrzyński, G. & Hetper, J. (1986). *Liebigs Ann. Chem.* pp. 980–991.
Oxford Diffraction (2002). *CrysAlis CCD* (Version 1.170) and *CrysAlis RED* (Version 1.170.16). Oxford Diffraction, Wrocław, Poland.
Padmanabhan, B., Dey, S., Khandelwal, B., Rao, G. S. & Singh, T. P. (1992). *Biopolymers*, **32**, 1271–1276.
Palmer, D. E., Pattaroni, C., Nunami, K., Chadha, R. K., Goodman, M., Wakamiya, T., Fukase, K., Horimoto, S., Kitazawa, M., Fujita, H., Kubo, A. & Shiba, T. (1992). *J. Am. Chem. Soc.* **114**, 5634–5642.
Perczel, A., Jákli, I., Foxman, B. M. & Fasman, G. D. (1996). *Biopolymers*, **38**, 723–732.
Piazzesi, A. M., Bardi, R., Crisma, M., Toniolo, C., Singh, M. & Chauhan, V. S. (1993). *Z. Kristallogr.* **207**, 25–32.
Rzeszotarska, B., Siodłak, D., Broda, M. A., Dybała, I. & Kozioł, A. E. (2002). *J. Pept. Res.* **59**, 79–89.
Sheldrick, G. M. (1990). *SHELXTL*. Siemens Analytical X-ray Instruments Inc., Madison, Wisconsin, USA.
Sheldrick, G. M. (1997). *SHELXS97* and *SHELXL97*. University of Göttingen, Germany.
Sigh, T. P. & Kaur, P. (1997). *Prog. Biophys. Mol. Biol.* **66**, 141–165.
Siodłak, D., Broda, M. A. & Rzeszotarska, B. (2004). *J. Mol. Struct. (Theochem)*, **668**, 75–85.
Świątek-Kozłowska, J., Brasuń, J., Chruściński, L., Chruścińska, E., Makowski, M. & Kozłowski, H. (2000). *New J. Chem.* **24**, 893–896.
Vass, E., Hollósi, M., Besson, F. & Buchet, R. (2003). *Chem. Rev.* **103**, 1917–1954.
Venkatachalam, C. M. (1968). *Biopolymers*, **6**, 1425–1436.
Zeng, X.-C. (2005). *Acta Cryst.* E**61**, o2958–o2960.